Contents lists available at ScienceDirect

Biochemistry and Biophysics Reports

Distinct roles in phagocytosis of the early and late increases of cell surface calreticulin induced by oxaliplatin

Kenju Matsusaka, Yutaro Azuma [*], Yuki Kaga, Saeka Uchida, Yuri Takebayashi, Takashi Tsuyama, Shusuke Tada

Department of Molecular Biology, Faculty of Pharmaceutical Sciences, Toho University, 2–2–1 Miyama, Funabashi, Chiba, 274–8510, Japan

ARTICLE INFO

ABSTRACT

Calreticulin (CRT), a chaperone typically located in the endoplasmic reticulum (ER), is known to translocate to the cell surface in response to anticancer drugs. Cell surface CRT (ecto-CRT) on apoptotic or pre-apoptotic cells serves as an "eat me" signal that can promote phagocytosis. In this study, we observed the biphasic (early transient and late sustained) increase of ecto-CRT on HT-29 cells after treatment with oxaliplatin (L-OHP). To investigate the role of ecto-CRT that accumulates in the early and late phases as "eat me" signals, we examined the phagocytosis of HT-29 cells by macrophage-like cells and dendritic cell (DC) -like cells prepared from THP-1 cells. The results indicated that the early ecto-CRT-expressed cells were phagocytosed by immature DC-like cells, and the late ecto-CRT-expressed cells were phagocytosed primarily by macrophage-like cells, while mature DC-like cells did not respond to the either class of ecto-CRT-expressed cells. Both types of phagocytotic events were inhibited by CRT Blocking Peptide, suggesting that such events depended on the ecto-CRT. Our results suggested that the early increase of ecto-CRT is related to phagocytosis as part of immunogenic cell death (ICD), while the late increase of ecto-CRT is related to the removal of apoptotic cells by macrophages.

1. Introduction

Calreticulin (CRT) is a chaperone protein located in the endoplasmic reticulum (ER); CRT is involved in the folding and quality control of proteins, and is associated with maintenance of calcium homeostasis in the ER. Although CRT is located primarily in the ER, CRT has been reported to show slight enrichment on the cell surface, and that cell surface CRT (ecto-CRT) plays roles in various processes such as regulation of focal adhesion, antigen presentation, and cell migration [1,2].

Recently, CRT was shown to translocate from the ER to the cell membrane during apoptosis, where the molecule functions as an "eat me" signal, promoting cellular engulfment by phagocytes [3,4]. In addition, it has been reported that treatment with certain chemotherapeutic agents (such as a synthetic anthracycline, mitoxantrone (MIT), and a platinum-based drug, oxaliplatin (L-OHP)) or irradiation of tumor cells induces the accumulation of ecto-CRT on the cells [5]. Previous studies also indicated that the increase in ecto-CRT is associated with ER

stress [5,6], and precedes various distinct morphological signs of apoptosis, such as phosphatidylserine (PS) exposure on the outer leaflet of the plasma membrane [7].

On the other hand, it has been reported that certain anticancer drugs, including MIT and L-OHP, induce immunogenic cell death (ICD), a process whereby an immune response against tumor cells is triggered [8, 9] and in which ecto-CRT plays an important role. In ICD, ecto-CRT on tumor cells serves as an "eat me" signal for phagocytosis by the antigen-presenting cells (APCs), followed by the presentation of tumor-specific antigens [4,9].

Previously, we reported that MIT induces a biphasic increase of ecto-CRT on HT-29 cells, a human colon cancer cell line, and that the early increase of ecto-CRT is related to ER stress, whereas the late phase of ecto-CRT accumulation is associated with apoptosis [10]. Thus, the physiological significance of the increases in ecto-CRT were assumed to differ between the early and the late stages. However, the specific roles of the early and the late increases of ecto-CRT remain unclear.

In this study, HT-29 cells were treated with L-OHP, which has been reported to induce ecto-CRT in some colon cancer cells [11,12], and the phagocytosis of the treated cells was investigated. Specifically, we analyzed the phagocytosis of the L-OHP-treated HT-29 cells by immature and mature DC-like cells and macrophage-like cells derived from THP-1 cells, and compared the responses to the early and late stages of L-OHP treatment. We also investigated the contribution of ecto-CRT to these phagocytotic events.

2. Materials and methods

2.1. Materials

Dulbecco's modified Eagle's medium (DMEM) and RPMI 1640 were obtained from Nissui Pharmaceutical Co. (Tokyo, Japan). Immuno-Cult™-ACF Dendritic Cell Medium was purchased from STEMCELL Technologies, Inc. (Vancouver, British Columbia, Canada). Fetal bovine serum (FBS) was purchased from Biosera (Nuaillé, France). Recombinant human interleukin-4 (rhIL-4) and recombinant human granulocyte-macrophage colony-stimulating factor (rhGM-CSF) were obtained from Pepro Tech, Inc. (Cranbury, NJ, USA). Recombinant human tumor necrosis factor-α (rhTNF-α) was obtained from R&D Systems, Inc. (Minneapolis, MN, USA). Acetyl-Asp-Glu-Val-Asp-aldehyde (Ac-DEVD-CHO, an inhibitor of caspase 3) was purchased from the Peptide Institute, Inc. (Osaka, Japan). Benzyloxycarbonyl-Ala-Thr-Ala-Asp-fluoromethyl ketone (Z-ATAD-FMK, an inhibitor of caspase 12) was purchased from MBL, Inc. (Woburn, MA, USA). Fluorescein isothiocyanate (FITC) -conjugated annexin V was purchased from Medical & Biological Laboratories Co. (Nagoya, Japan). Phosphatidylcholine (PC), phosphatidylserine (PS), and oxaliplatin (L-OHP) were obtained from Wako Pure Chemical Industries (Osaka, Japan). 7-Amino-actinomycin D (7-AAD), phorbol 12-myristate 13-acetate (PMA), and the PKH26 Red Fluorescent Cell Linker kit were purchased from Sigma-Aldrich Co. (St. Louis, MO, USA). Anti-calreticulin antibody (FMC75) was obtained from Enzo Life Sciences, Inc. (Farmingdale, NY, USA). Anti-CD80 antibody (F-7), anti-CD86 antibody (BU63), FITC-conjugated anti-CD11b antibody (2LPM19c), and Alexa Fluor® 488-conjugated anti-CD11c antibody (3.9) were purchased from Santa Cruz Biotechnology, Inc. (Dallas, TX, USA). FITC-conjugated anti-CD14 antibody (UCHM1) was obtained from AbD Serotec. (Raleigh, NC, USA). The secondary antibody, Alexa Fluor® 488-conjugated goat anti-mouse IgG (H+L) antibody (A11001) was purchased from Invitrogen Co. (Carlsbad, CA, USA). Blocking One was purchased from Nacalai Tesque, Inc. (Kyoto, Japan). Calreticulin Blocking Peptide (synthetic peptide mapping to the C-terminus of human calreticulin) was obtained from BioVision, Inc. (Milpitas, CA, USA). All other chemicals were purchased from Sigma-Aldrich Co., Nacalai Tesque, Inc., or Wako Pure Chemical Industries.

2.2. Cell lines and culture conditions

The human colon adenocarcinoma cell line HT-29 was obtained from the American Type Culture Collection (Manassas, VA, USA); the human monocytic cell line THP-1 was obtained from Japanese Collection of Research Bioresources (Tokyo, Japan). HT-29 cells were maintained in DMEM supplemented with 10% heat-inactivated FBS, 0.3 mg/mL glutamine, 100 U/mL penicillin, and 100 μg/mL streptomycin at 37 °C under a humidified atmosphere containing 5% CO_2. THP-1 cells were maintained in RPMI 1640 supplemented with 10% heat-inactivated FBS under similar conditions.

2.3. Treatment of L-OHP and flow cytometric analysis of cell surface CRT

HT-29 cells were treated with 20 μM or 200 μM L-OHP in 10% FBS/DMEM for 0–48 h at 37 °C under 5% CO_2. The attached HT29 cells were washed with PBS, detached with 0.02% EDTA, and collected by centrifugation. The cell surface CRT of the collected HT29 cells were analyzed by flow cytometry. Specifically, L-OHP-treated cells were incubated with 10 μg/mL anti-human CRT antibody in 1% bovine serum albumin/phosphate buffered saline (BSA/PBS) for 30 min on ice. After two rounds of washing with 1% BSA/PBS, cells were incubated with 10 μg/mL Alexa Fluor® 488-conjugated anti-mouse IgG antibody in 1% BSA/PBS for 30 min on ice. After two rounds of washing with 1% BSA/PBS, permeated cells were stained with 0.25 μg/mL 7-AAD in 1% BSA/PBS for 5 min on ice. The fluorescence intensities of Alexa Fluor® 488 on the 7-AAD-negative cells were analyzed using a BD FACS Calibur™ flow cytometer (Becton Dickinson Co., USA). Analysis of mean fluorescence intensity (MFI) was performed using Flow Jo software (FlowJo, LLC, Ashland OR, USA). The MFI of cells treated with 1% BSA/PBS instead of the primary antibody was subtracted as the background. To inhibit caspase 3 or caspase 12, 100 μM Ac-DEVD-CHO (an inhibitor of caspase 3) or 5 μM Z-ATAD-FMK (an inhibitor of caspase 12) (respectively) was added to the culture medium.

2.4. Flow cytometric analysis of cell surface PS

For measurement of PS on the cell surface, cells were treated with 5 μg/mL FITC-conjugated annexin V in binding buffer (10 mM HEPES NaOH, pH 7.4, 140 mM NaCl, 2.5 mM $CaCl_2$) at room temperature in the dark for 10 min. After two rounds of washing with binding buffer, the fluorescence intensities of FITC on the cells were analyzed by flow cytometry.

2.5. Preparation of macrophage-like cells and DC-like cells

THP-1 cells (5×10^5 cells/mL) were treated with 100 nM PMA in 10% FBS/RPMI 1640 for 48 h at 37 °C under 5% CO_2 to induce differentiation into macrophage-like cells. Differentiation into dendritic cell (DC) -like cells was performed using a slight modification of the procedure described by Berges et al. [13]. To induce differentiation into immature DCs, THP-1 cells (5×10^5 cells/mL) were treated with 35 ng/mL rhIL-4 and 50 ng/mL rhGM-CSF in ImmunoCult™-ACF Dendritic Cell Medium for 5 days at 37 °C under 5% CO_2. To induce differentiation into mature DCs, immature DCs were treated with 35 ng/mL rhIL-4, 50 ng/mL rhGM-CSF, and 40 ng/mL rhTNF-α for an additional 2 days under similar conditions.

2.6. Flow cytometric analysis of cell surface CD antigens

The abundance of cell surface CD antigens on THP-1 cells treated with PMA or cytokines was analyzed by flow cytometry. The cell surface CD11b, CD11c, and CD14 were analyzed as specific macrophage markers, and the cell surface CD80 and CD86 were analyzed as specific DC markers. For the detection of the macrophage markers, cells were incubated with 10 μg/mL of fluorescent labeled antibody (FITC-anti CD11b antibody, Alexa Fluor® 488-anti CD11c antibody, or FITC-anti CD14 antibody) in 1% BSA/PBS for 30 min on ice. The cells were washed twice and analyzed for fluorescence intensities by flow cytometry. For the detection of the DC markers, cells were incubated with 10 μg/mL of the primary antibody (anti CD80 antibody or anti CD86 IgG antibody) in 1% BSA/PBS for 30 min on ice. After two rounds of washing with 1% BSA/PBS, the cells were incubated with 10 μg/mL Alexa Fluor® 488-anti-mouse IgG antibody in 1% BSA/PBS for 30 min on ice. The cells were washed twice and analyzed for the fluorescence intensities of Alexa Fluor® 488 by flow cytometry. The fluorescence intensity of the cells treated with 1% BSA/PBS instead of the antibodies was subtracted as background.

2.7. Preparation of PS liposomes

Liposomes containing PS and PC were prepared using a slight modification of the procedure described by Fadok et al. [14]. Specifically, PS liposomes were generated by suspending PS and PC

(separately) in chloroform/methanol (9:1) and then adding the suspensions to glass tubes at relative concentrations of 70% PC and 30% PS. The solvent was evaporated under N_2 gas, and the lipids were resuspended in HEPES buffer (10 mM HEPES NaOH, pH 7.4, 140 mM NaCl, 2.5 mM $CaCl_2$) by vigorous mixing. The mixtures subsequently were sonicated for 5 min on ice. Prepared liposomes were suspended in the relevant growth medium for use in the phagocytosis inhibitory assay.

2.8. Phagocytosis assay

L-OHP-treated HT-29 cells were collected and stained with PKH-26 according to the manufacturer's protocol. To block non-specific phagocytic reactions, PKH26-stained HT-29 cells were treated with Blocking One for 10 min at room temperature and washed with PBS. PKH26-stained HT-29 cells were added to THP-1-derived macrophages or THP-1-derived DCs, and the mixtures were incubated for 30 min at 37 °C under 5% CO_2. For the inhibition of phagocytosis, 10 μg/mL CRT Blocking Peptide or 50 μM PS liposome was included directly in the medium. After incubation, culture medium was removed and adherent phagocytes were washed with PBS. To remove non-specifically adhered HT-29 cells, the cells were treated with 0.02% EDTA/PBS for 1 min at room temperature and further washed with PBS. Then, the phagocytes were treated with 0.02% EDTA/PBS for 10 min at 37 °C to generate a single-cell suspension. These phagocytes were analyzed by flow cytometry, and the proportion of cells showing higher fluorescence intensity was measured as cells engulfed PKH26-stained HT-29 cells to determine the phagocytosis ratio.

2.9. Statistical analyses

All data are presented as the mean ± S.D. from independent experiments. To evaluate statistical significance, the two-tailed non-paired Student's t-test was used in studies comparing two groups, while two-tailed one-way variance analysis (ANOVA) followed by Dunnett's multiple comparison test was used to evaluate data from more than two groups. All statistical analyses were performed with EZR (Saitama Medical Center, Jichi Medical University, Saitama, Japan), which is a graphical user interface for R (The R Foundation for Statistical Computing, Vienna, Austria) [15]. A value of $P < 0.05$ was considered statistically significant.

3. Results

3.1. L-OHP-induces accumulation of cell surface CRT (ecto-CRT) in HT-29 cells

Given that oxaliplatin (L-OHP) has been reported to induce an increase in the level of cell surface CRT (ecto-CRT) in human colon cancer cell lines [11,12], we treated HT-29 cells with L-OHP and examined the accumulation of ecto-CRT on HT-29 cells. L-OHP induced a biphasic increase of ecto-CRT that was observed as a transient early increase, peaking at 4 h, and a late increase, after 24 h (Fig. 1). We reported previously that a similar biphasic increase of ecto-CRT is seen on MIT-treated HT-29 cells, including an early increase related to ER stress and a late increase associated with apoptosis [10]. On the other hand, L-OHP is also known to induce ER stress, which has been reported to be associated with an increase in ecto-CRT [5]. Therefore, we studied the effects of inhibitors of caspase 3 and caspase 12, which are respectively involved in apoptosis and ER stress, on the increase of ecto-CRT in L-OHP-treated HT-29 cells. As shown in Fig. 2A, a caspase 3 inhibitor attenuated the increase of ecto-CRT on HT-29 cells after a 48-h treatment with L-OHP, whereas a caspase 3 inhibitor did not affect the increase of ecto-CRT on L-OHP-treated HT-29 cells at 4 h. On the other hand, a caspase 12 inhibitor suppressed the increase of ecto-CRT on L-OHP-treated HT-29 cells at 4 h (Fig. 2B). In addition, we observed phosphorylation of the α-subunit of eukaryotic initiation factor 2 (eIF2-α) in HT-29 cells within 6 h after L-OHP treatment (data not shown). These results suggested that L-OHP induces an ER stress-associated early increase of ecto-CRT, while the late increase of ecto-CRT related to the caspase 3 activation of apoptosis.
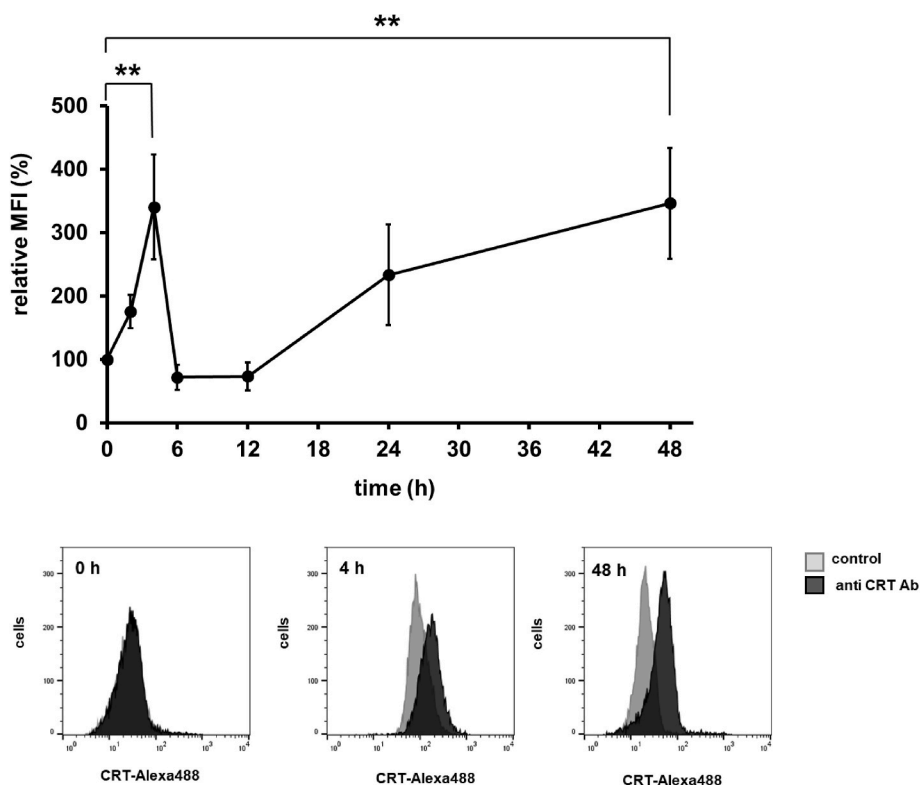

Fig. 1. Alteration of ecto-CRT on the L-OHP-treated HT-29 cells. HT-29 cells were treated with oxaliplatin (L-OHP) (20 μM) for 0–48 h, and calreticulin (CRT) accumulation on the surface of intact cells was measured by flow cytometry as described in Materials and Methods. The data are expressed as percentages of the values for untreated control HT29 cells. The data are presented as mean ± S.D. ($n = 3$); asterisks indicate significance compared with 0 h (**$p < 0.01$; two-tailed one-way variance analysis (ANOVA) with post hoc Dunnett's multiple comparison test). The gray histograms show background controls, and the black histograms show the binding of anti CRT antibody.
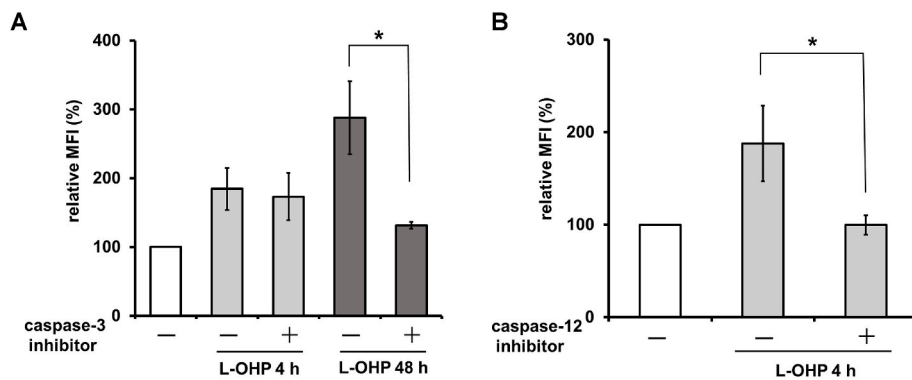
Fig. 2. Effects of caspase inhibitor on ecto-CRT accumulation in L-OHP-treated HT-29 cells. (A) HT-29 cells were treated with L-OHP (20 μM) for 4 or 48 h in the presence or absence of a caspase 3 inhibitor (Ac-DEVD-CHO) (100 μM), and CRT accumulation on the cells was measured. (B) HT-29 cells were treated with L-OHP (20 μM) for 4 h in the presence or absence of the caspase 12 inhibitor (Z-ATAD-FMK) (5 μM), and CRT accumulation on the cells was measured. The data are expressed as percentages of the values for untreated control HT29 cells. The data are presented as mean ± S.D. ($n = 3$) and differences between two groups were compared (*$p < 0.05$; two-tailed non-paired Student's t-test).

3.2. Induction of differentiation of THP-1 cells into macrophage-like cells and dendritic cell-like cells

Cells of the human monocytic cell line THP-1 are known to differentiate into macrophage-like cells following treatment with phorbol 12-myristate 13-acetate (PMA) [16], and into immature dendritic cell (DC)-like cells following treatment with GM-CSF and IL-4. In addition, the immature DC-like cells can be induced to developed into mature DC-like cells by additional treatment with TNF-α [13]. Therefore, we treated THP-1 cells with PMA or cytokines and determined the abundance of cell surface antigens specific for macrophages or DCs on the PMA-treated or cytokine-treated THP-1 cells. The abundance of cell surface markers CD11b, CD11c, and CD14 were increased on the PMA-treated THP-1 cells, whereas the abundance of CD80 and CD86 were not changed (Fig. 3). On the other hand, the abundance of cell surface markers CD11b, CD80, and CD86 were increased on the GM-CSF- and IL-4-treated THP-1 cells, while that of CD14 was decreased. These changes in the cell surface antigens on the GM-CSF- and IL-4-treated THP-1 cells were enhanced by subsequent treatment with TNF-α (Fig. 3B). Thus, THP-1 cells acquired the characteristics of macrophages or of DCs (immature and mature) when cultured with PMA or cytokines, respectively.

3.3. The phagocytosis of L-OHP-treated HT-29 cells by phagocytes differentiated from THP-1 cells

To investigate phagocytosis of L-OHP-treated HT-29 cells by macrophages, immature DCs, and mature DCs, HT-29 cells treated with L-

OHP for 4 or 48 h were co-incubated with each phagocytic cells derived from THP-1 (Fig. 4). HT-29 cells that had been exposed to L-OHP for 4 h were phagocytosed by immature DC-like cells, and the degree of phagocytosis of the L-OHP-treated cells was considerably higher than that of untreated HT-29 cells. Little phagocytosis of treatment-naïve HT-29 cells was seen with macrophage-like cells or mature DC-like cells, and the level of phagocytosis was not significantly increased after 4-h treatment of HT-29 cells with L-OHP (Fig. 4A). On the other hand, phagocytosis of HT-29 cells by macrophage-like cells increased significantly after 48-h treatment of HT-29 cells with L-OHP; however, this treatment of HT-29 cells did not potentiate phagocytosis by immature DC-like cells (Fig. 4B). These results indicated that immature DC-like cells and macrophage-like cells preferentially phagocytose distinct target cells. We hypothesize that phagocytosis of cells in the early stage of L-OHP treatment plays a different role in cancer immunity that does phagocytosis of cells in the late stage of L-OHP treatment.

3.4. The contribution of ecto-CRT and cell surface PS to phagocytosis of L-OHP-treated HT-29 cells

Phosphatidylserine (PS), which is almost totally confined to the inner leaflet of the normal plasma membrane, moves to the outer leaflet during apoptosis. Therefore, cell surface PS is a characteristic marker of apoptosis and reportedly provides an "eat me" signal on apoptotic cells. We examined cell surface PS, in addition to ecto-CRT, on HT-29 cells after 4-h or 48-h treatment with L-OHP. As shown in Fig. 5, significant increases in ecto-CRT were observed on HT-29 cells treated with L-OHP, whether for 4 or 48 h, whereas the increase in cell surface PS was
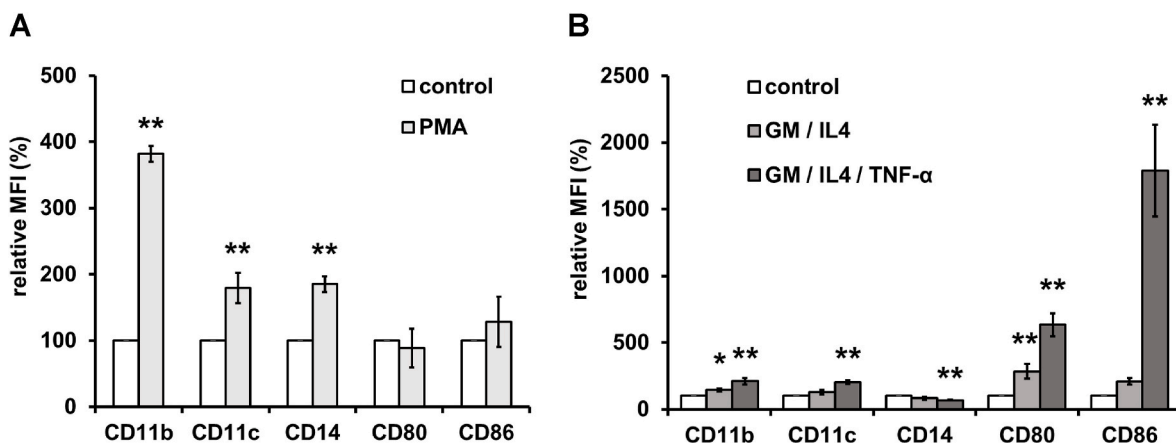

Fig. 3. Flow cytometric analysis of cell surface antigen on PMA- or cytokine-treated THP-1 cells. THP-1 cells were treated with (A) phorbol 12-myristate 13-acetate (PMA) for 2 days, or (B) granulocyte-macrophage colony-stimulating factor (GM-CSF) and interleukin-4 (IL-4) for 5 days or GM-CSF, IL-4, and tumor necrosis factor-α (TNF-α) for 7 days. CD11b, CD11c, CD14, CD80, and CD86 on the cell surface were measured by flow cytometry as described in Materials and Methods. The data are expressed as percentages of the values for untreated control THP-1 cells. The data are presented as mean ± S.D. ($n = 3$) and asterisks indicate significance compared with untreated control cells (*$p < 0.05$, **$p < 0.01$; two-tailed one-way variance analysis (ANOVA) with post hoc Dunnett's multiple comparison test).
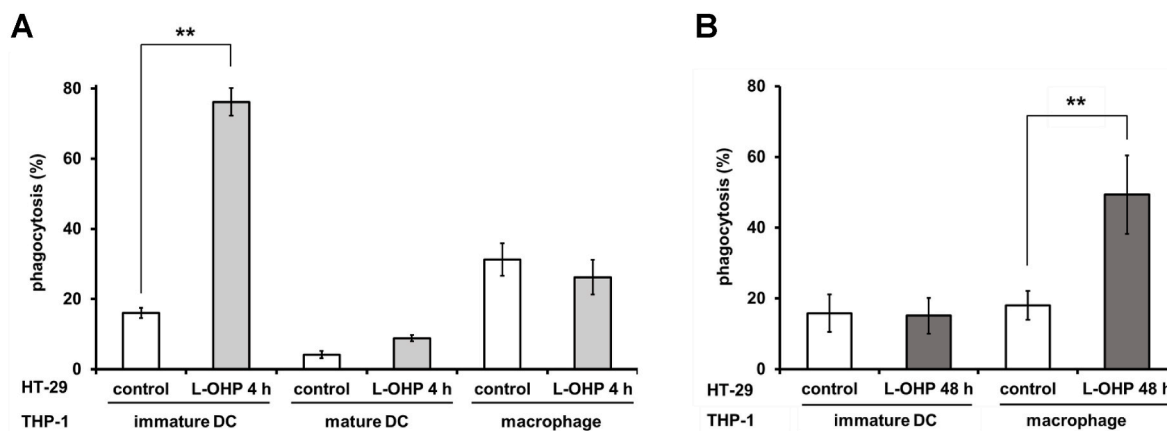
Fig. 4. Phagocytosis of L-OHP-treated HT-29 cells by immature DC-like cells, mature DC-like cells, and macrophage-like cells. HT-29 cells were treated with oxaliplatin (L-OHP) (200 μM) for (A) 4 h or (B) 48 h, and stained with PKH26. Stained HT-29 cells were co-incubated with immature DC-like cells, mature DC-like cells, or macrophage-like cells for 30 min. Phagocytosis during the co-incubation was assayed as described in Materials and Methods. The data are presented as mean ± S. D. (n = 3) and asterisks indicate significance compared to untreated control cells (**p < 0.01; two-tailed non-paired Student's t-test).
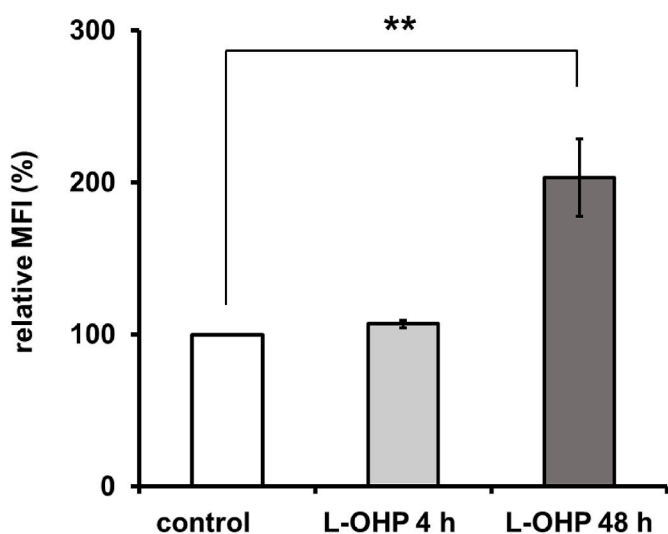

Fig. 5. Cell surface PS on L-OHP-treated HT-29 cells. HT-29 cells were treated with oxaliplatin (L-OHP) for 4 or 48 h. (A) calreticulin (CRT) or (B) phosphatidylserine (PS) accumulation on the cell surface were measured by flow cytometry as described in Materials and Methods. The data are expressed as percentages of the values for untreated control HT-29 cells. The data are presented as mean ± S.D. (n = 3), and asterisks indicate significance compared with untreated control cells (*p < 0.05, **p < 0.01; two-tailed one-way variance analysis (ANOVA) with post hoc Dunnett's multiple comparison test).

observed only on HT-29 cells treated with L-OHP for 48 h. These results indicated that HT-29 cells subjected to 4-h or 48-h-treatment with L-OHP could be considered pre-apoptotic or apoptotic, respectively. Next, we investigated the effects of CRT Blocking Peptide and PS liposomes on the phagocytosis of L-OHP-treated HT-29 cells; these experiments were expected to clarify the involvement of ecto-CRT and cell surface PS in these phagocytotic events. The fraction of HT-29 cells phagocytosed by immature DC-like cells was increased after a 4-h L-OHP treatment, and this effect was significantly suppressed by the addition of CRT Blocking Peptide (Fig. 6A). These results suggested that the early increase of ecto-CRT plays a role as an "eat me" signal for phagocytosis by immature DC-like cells. In case of the phagocytosis by macrophage-like cells of HT-29 cells after 48-h L-OHP treatment, the increase was significantly suppressed by CRT Blocking Peptide and (separately) by PS liposomes (Fig. 6B). These results suggested that the late increase of ecto-CRT, as well as that of cell surface PS, is involved in phagocytosis by

macrophage-like cells.

4. Discussion

The CRT chaperone protein normally is located in the ER, but is known to move to the cell surface as an "eat me" signal for phagocytosis when cells are treated with certain anticancer drugs [4]. In our previous study, a biphasic increase of ecto-CRT was observed on HT-29 cells after treatment with MIT [10]. In the present study, we observed that L-OHP treatment of HT-29 cells also induces an early, transient, ER stress-related increase in ecto-CRT as well as a late, persistent, apoptosis-related increase in ecto-CRT (Figs. 1 and 2). Although the ecto-CRT is known to play an important role in the phagocytotic removal of apoptotic cells and immunogenic cell death (ICD) in immunotherapy as "eat me" signal [3,4], it was considered that differences in ICD of ecto-CRT between apoptotic cells and non-apoptotic cells. Therefore, we studied the physiological significance of the early transient and late persistent increases in ecto-CRT as "eat me" signals for phagocytosis using immature and mature DC-like cells or macrophage-like cells differentiated from THP-1. HT-29 cells after 4- and 48-h L-OHP treatment were more readily phagocytosed than untreated HT-29 cells, and this phagocytosis was attenuated in the presence of CRT Blocking Peptide (Fig. 6). This peptide was used to inhibit the cellular functions of CRT [12,17], suggesting that both increases in ecto-CRT were relevant to phagocytosis (Fig. 6). However, cells with the early increase in ecto-CRT were phagocytosed by immature DC-like cells, while the cells at the later stage were phagocytosed primarily by macrophage-like cells (Fig. 4).

In ICD, the ecto-CRT-mediated phagocytosis of tumor cells by immature DCs induces tumor antigen presentation to T cells [18,19]. After phagocytosis of cancer cells, immature DCs differentiate into mature DCs, enabling the elicitation of potent anticancer immunity. We conjecture that the early increase in ecto-CRT observed in the present study contributes to tumor antigen presentation by DCs.

The early increase of ecto-CRT on HT-29 cells treated with L-OHP was transient and exhibited a rapid subsequent decrease (Fig. 1). Recently, CRT has been reported to accumulate on the surface of Jurkat cells undergoing UV-induced apoptosis; the accumulated ecto-CRT subsequently is released from the cells [20]. We therefore suspect that the ecto-CRT observed to accumulate on the surface of HT-29 cells similarly is released subsequently from the cells. Soluble CRT released from cells, as well as recombinant CRT, have been reported to act as damage-associated molecular patterns (DAMPs) to promote DC maturation [21]. Taken together, these results suggest that the early increase in ecto-CRT serves as an "eat me" signal for phagocytosis by immature
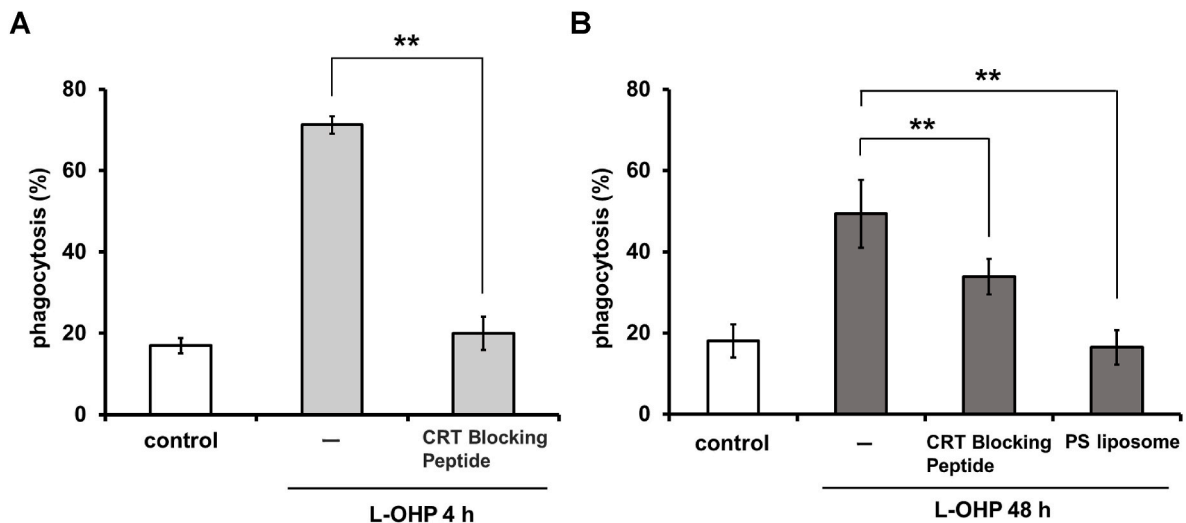
Fig. 6. Effect of CRT Blocking Peptide and PS liposomes on the phagocytosis of L-OHP-treated HT-29 cells. After treatment with oxaliplatin (L-OHP) and staining with PKH26, HT-29 cells were co-incubated with (A) immature DC-like cells, or (B) macrophage-like cells for 30 min in the presence or absence of the CRT Blocking Peptide or PS liposomes. Phagocytosis during the co-incubation was assayed as described in Materials and Methods. The data are presented as mean ± S.D. ($n = 3$), and asterisks indicate significance compared with L-OHP-treated HT-29 cells in the absence of CRT Blocking Peptide and PS liposomes (**$p < 0.01$; (A) two-tailed non-paired Student's t-test, (B) two-tailed one-way variance analysis (ANOVA) with post hoc Dunnett's multiple comparison test).

DCs, while the subsequent liberation of CRT from cells induces maturation of DCs; both steps are expected to contribute to tumor-antigen presentation, thereby facilitating efficient ICD.

After 48-h treatment with L-OHP, PS, as well as ecto-CRT, accumulates on the cell surface of HT-29 cells (Fig. 5B). The HT-29 cells with the later increase of ecto-CRT were phagocytosed by macrophage-like cells, and this phagocytosis was attenuated in the presence of PS liposomes (Fig. 6B). These results indicate that HT-29 cells treated with L-OHP for 48 h undergo apoptotic processes resulting in the accumulation of PS at the cell surface, which also serves as an "eat me" signal. Recently, it has been reported that ecto-CRT on apoptotic cells and externalized PS may co-localize and synergize with other PS-binding factors to enhance phagocytosis of apoptotic cells [22,23]. In the present study, macrophage-like cells preferentially phagocytosed HT-29 cells treated with L-OHP for 48 h (compared to cells treated for 4 h), although high levels of ecto-CRT were expressed by both classes of cells (Fig. 4). These results suggested that the later increase of ecto-CRT likely synergizes with the exposure of PS, enhancing the function of ecto-CRT as an "eat me" signal for phagocytosis by macrophages.

Our observations suggest that the biphasic increase in ecto-CRT may be a mechanism for enhancing anti-tumor immunity. Recently, it has been shown that ecto-CRT-related ICDs are even more effective in cancer immunological cancer therapy when combined with various chemotherapeutic agent [6,8,24,25]. Therefore, elucidation of the mechanisms and functions of the relocation of CRT is expected to lead to therapeutics that enhance immunogenicity against tumor cells, facilitating the removal of apoptotic tumor cells.

Declaration of interests

The authors declare that they have no known competing financial interests or personal relationships that could have appeared to influence the work reported in this paper.

References

[1] M. Michalak, J. Groenendyk, E. Szabo, L.I. Gold, M. Opas, Calreticulin, a multi-process calcium-buffering chaperone of the endoplasmic reticulum, Biochem. J. 417 (2009) 651–666.
[2] L.I. Gold, P. Eggleton, M.T. Sweetwyne, L.B. Van Duyn, M.R. Greives, S. Naylor, M. Michalak, J.E. Murphy-Ullrich, Calreticulin: non-endoplasmic reticulum functions in physiology and disease, Faseb. J. 24 (2010) 665–683.
[3] S.J. Gardai, K.A. McPhillips, S.C. Frasch, W.J. Janssen, A. Starefeldt, J.E. Murphy-Ullrich, D.L. Bratton, P. Oldenborg, M. Michalak, P.M. Henson, Cell-surface calreticulin initiates clearance of viable or apoptotic cells through trans-activation of LRP on the phagocyte, Cell 123 (2005) 321–334.
[4] M. Obeid, A. Tesniere, F. Ghiringhelli, G.M. Fimia, L. Apetoh, J. Perfettini, M. Castedo, G. Mignot, T. Panaretakis, N. Casares, D. Métivier, N. Larochette, P. van Endert, F. Ciccosanti, M. Piacentini, L. Zitvogel, G. Kroemer, Calreticulin exposure dictates the immunogenicity of cancer cell death, Nat. Med. 13 (2007) 54–61.
[5] T. Panaretakis, O. Kepp, U. Brockmeier, A. Tesniere, A. Bjorklund, D.C. Chapman, M. Durchschlag, N. Joza, G. Pierron, P. van Endert, J. Yuan, L. Zitvogel, F. Madeo, D.B. Williams, G. Kroemer, Mechanisms of pre-apoptotic calreticulin exposure in immunogenic cell death, EMBO J. 28 (2009) 578–590.
[6] L. Zitvogel, O. Kepp, L. Senovilla, L. Menger, N. Chaput, G. Kroemer, Immunogenic tumor cell death for optimal anticancer therapy: the calreticulin exposure pathway, Clin. Cancer Res. 16 (2010) 3100–3104.
[7] R. Tufi, T. Panaretakis, K. Bianchi, A. Criollo, B. Fazi, F. Di Sano, A. Tesniere, O. Kepp, P. Paterlini-Brechot, L. Zitvogel, M. Piacentini, G. Szabadkai, G. Kroemer, Reduction of endoplasmic reticulum Ca2+ levels favors plasma membrane surface exposure of calreticulin, Cell Death Differ. 15 (2008) 274–282.
[8] L. Bezu, L.C. Gomes-de-Silva, H. Dewitte, K. Breckpot, J. Fucikova, R. Spisek, L. Galluzzi, O. Kepp, G. Kroemer, Combinatorial strategies for the induction of immunogenic cell death, Front. Immunol. 6 (2015) 187.
[9] L. Bezu, A. Wu Chuang, J. Humeau, G. Kroemer, O. Kepp, Quantification of eIF2alpha phosphorylation during immunogenic cell death, Methods Enzymol. 629 (2019) 53–69.
[10] Y. Azuma, K. Suzuki, K. Higai, K. Matsumoto, S. Tada, Biphasic increases of cell surface calreticulin following treatment with mitoxantrone, Biol. Pharm. Bull. 43 (2020) 1595–1599.
[11] A. Tesniere, F. Schlemmer, V. Boige, O. Kepp, I. Martins, F. Ghiringhelli, L. Aymeric, M. Michaud, L. Apetoh, L. Barault, J. Mendiboure, J.-P. Pignon, V. Jooste, P. van Endert, M. Ducreux, L. Zitvogel, F. Piard, G. Kroemer, Immunogenic death of colon cancer cells treated with oxaliplatin, Oncogene 29 (2010) 482–491.
[12] S. Di Blasio, I.M.N. Wortel, Diede A.G. van Bladel, L.E. de Vries, T. Duiveman-de Boer, K. Worah, N. de Haas, S.I. Buschow, I.Jolanda M. de Vries, C.G. Figdor, S.V. Hato, Human CD1c(+) DCs are critical cellular mediators of immune responses induced by immunogenic cell death, OncoImmunology 5 (2016), e1192739.
[13] C. Berges, C. Naujokat, S. Tinapp, H. Wieczorek, A. Höh, M. Sadeghi, G. Opelz, V. Daniel, A cell line model for the differentiation of human dendritic cells, Biochem. Biophys. Res. Commun. 333 (2005) 896–907.
[14] V.A. Fadok, D.R. Voelker, P.A. Campbell, J.J. Cohen, D.L. Bratton, P.M. Henson, Exposure of phosphatidylserine on the surface of apoptotic lymphocytes triggers specific recognition and removal by macrophages, J. Immunol. 148 (1992) 2207–2216.
[15] Y. Kanda, Investigation of the freely available easy-to-use software 'EZR' for medical statistics, Bone Marrow Transplant. 48 (2013) 452–458.
[16] H. Schwende, E. Fitzke, P. Ambs, P. Dieter, Differences in the state of differentiation of THP-1 cells induced by phorbol ester and 1,25-dihydroxyvitamin D3, J. Leukoc. Biol. 59 (1996) 555–561.
[17] M.P. Chao, S. Jaiswal, R. Weissman-Tsukamoto, A.A. Alizadeh, A.J. Gentles, J. Volkmer, K. Weiskopf, S.B. Willingham, T. Raveh, C.Y. Park, R. Majeti, I.L. Weissman, Calreticulin is the dominant pro-phagocytic signal on multiple

human cancers and is counterbalanced by CD47, Sci. Transl. Med. 22 (2010) 63ra94.

[18] J. Zhou, G. Wang, Y. Chen, H. Wang, Y. Hua, Z. Cai, Immunogenic cell death in cancer therapy: present and emerging inducers, J. Cell Mol. Med. 23 (2019) 4854–4865.

[19] M. Kielbik, I. Szulc-Kielbik, M. Klink, Calreticulin-multifunctional chaperone in immunogenic cell death: potential significance as a prognostic biomarker in ovarian cancer patients, Cells 10 (2021).

[20] R. Osman, P. Tacnet-Delorme, J. Kleman, A. Millet, P. Frachet, Calreticulin release at an early stage of death modulates the clearance by macrophages of apoptotic cells, Front. Immunol. 8 (2017) 1034.

[21] A. Bajor, S. Tischer, C. Figueiredo, M. Wittmann, S. Immenschuh, R. Blasczyk, B. Eiz-Vesper, Modulatory role of calreticulin as chaperokine for dendritic cell-based immunotherapy, Clin. Exp. Immunol. 165 (2011) 220–234.

[22] S.J. Wijeyesakere, S.K. Bedi, D. Huynh, M. Raghavan, The C-terminal acidic region of calreticulin mediates phosphatidylserine binding and apoptotic cell phagocytosis, J. Immunol. 196 (2016) 3896–3909, 1950).

[23] J.M. Tarr, P.J. Young, R. Morse, D.J. Shaw, R. Haigh, P.G. Petrov, S.J. Johnson, P. G. Winyard, P. Eggleton, A mechanism of release of calreticulin from cells during apoptosis, J. Mol. Biol. 401 (2010) 799–812.

[24] Y. Zhang, R. Thangam, S.H. You, R.D. Sultonova, A. Venu, J.J. Min, Y. Hong, Engineering calreticulin-targeting monobodies to detect immunogenic cell death in cancer chemotherapy, Cancers 13 (2021) 2801.

[25] J. Fucikova, R. Spisek, G. Kroemer, L. Galluzzi, Calreticulin and cancer, Cell Res. 31 (2021) 5–16.